

Preparation of Al₂O₃/SiC Nanocomposites with In-Situ Formed SiC

Jürgen Hopf*, Mesut Aslan*, Helmut Schmidt**

received: 04.10.2006; revised: 02.02.2006; accepted: 01.03.2006

Keywords: Al₂O₃, SiC, nanocomposites, mechanical properties, in situ formation

Abstract

Powder mixtures containing Al₂O₃, SiO₂ and carbon black were calcined at 1625°C to form nanoscaled SiC within Al₂O₃ by means of the carbothermal reduction of SiO₂. The prepared powders contained 5 and 10 vol. % SiC. These powders were densified by hot pressing, and composite ceramics with densities up to 99 % obtained. Microstructural analyses of the hot-pressed composites showed a homogeneous distribution of SiC particles with a particle size mainly under 100 nm. The fracture mode was intragranular. The fracture toughness determined by the ICL method using the Niihara approach for Palmqvist cracks was in the range of 5 MPa·m^{0.5}. The fracture strength determined in a four-point bending test was around 540 MPa for the hot-pressed samples and around 630 MPa for the hot-pressed and post-annealed samples.

1 Introduction

Since the early 1990s ceramic-ceramic nanocomposites have attracted considerable interest because of their mechanical behaviour at high temperatures, e.g. for use as cutting tools. Niihara [1] reported a strength enhancement from 320 MPa to 1050 MPa for alumina reinforced with 5 vol. % silicon carbide and an increase in fracture toughness from 3,2 MPa·m^{0.5} to 4,7 MPa·m^{0.5}. A lot of work has been done on this system [2-5], but Niihara's values have remained elusive, although an increase in fracture strength is undisputed as, for example, the results of Sternitzke et al. [4] (539...738 MPa, determined in four-point bending tests) and Gao et al. [5] (spark plasma sintering; about 1000 MPa in three-point bending tests) demonstrate. Working on the widely spread assumption that the distribution of the second-phase particles plays an important role in strength enhancement, many researchers have focused on the in situ formation of either the matrix phase or the reinforcement second phase by sol-gel-methods [6-8], precipitation reactions [7] or the pyrolysis of Si-containing organic precursors [9].

The mechanism(s) behind this strength enhancement remain the subject of discussion. There are three phenomena that can be made responsible for the strength increase [10]:

- the reduction of the critical flaw size by refinement of the matrix grains [2], by a dislocation network [1] or by a reduction of processing flaws [4]
- the increase in fracture toughness ("K-mechanisms") [10]
- mechanisms based on the strengthening of grain boundaries [2,11].

Strengthening of grain boundaries as a result of internal stresses is widely accepted because in the case of the composites, there is a change in fracture mode from intergranular for alumina to intragranular for the composites.

Another influence to be taken into account is the method of preparing the samples for testing their fracture strength. Poorteman et al. [3] reported on samples with 5 vol. % SiC, where the samples had been prepared by two different methods: one method involved polishing the tensile side and bevelling the edges, the other included an additional polishing of the lateral sides of the bars. The latter route led to strength values of 800 MPa in three-point bending tests (samples prepared by the first route reached about 600 MPa).

The aim of this work was to develop a new processing route in order to realize a homogenous distribution of reinforcing SiC particles. The fine-grained silicon carbide powder within the alumina matrix will be formed by the carbothermal reduction of nanoscaled silica by carbon black, both added to the alumina. The reaction of silicon dioxide and carbon black after Equation (1) is commonly known to form silicon carbide, but has never been used to produce alumina/silicon carbide nanocomposites.

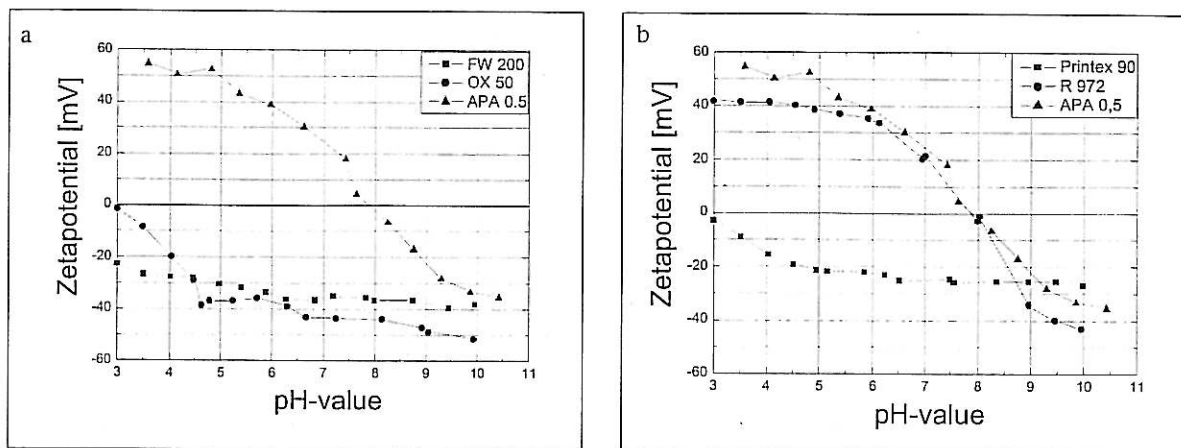


Thermodynamically the reaction starts at temperatures above 1530°C. Accompanied by various reaction stages, the overall reaction stops when either the carbon or silicon dioxide is completely consumed [12]. The preparation of homogeneous slurries requires the optimization of dispersion and homogenization of the starting powders in aqueous slurries, which is achieved by adjustment of the pH value depending on the different zeta potentials of the nanoscaled precursor powders (Fig. 1). The homogenization of nanoscaled components in aqueous slurries can be

* Leibniz-Institut für Neue Materialien gem. GmbH, Im Stadtwald, Geb. D2.2, D-66123 Saarbrücken;

** Universität des Saarlandes, Lehrstuhl für Neue Materialien, Beethovenstrasse, Zeile 4, D-66125 Saarbrücken-Dudweiler

Fig. 1
pH-value vs. zeta-potential for the powders APA 0,5/ OX 50/FW 200 (left) and for APA 0,5/R 972/FW 200 (right)



carried out by two different methods, one is a "coating route" when using components with opposite surface charge, the second is a polydispersed slurry when the components have equal surface charge.

2 Experimental Procedure

The starting powders were α -Al₂O₃ as the matrix phase (Ceralox APA 0,5 MgO, average particle size 400 nm, specific surface area 7 m²/g, *Condea*) for both homogenization methods, SiO₂ (Aerosil R972, specific surface area 110 m²/g, *Degussa*) and carbon black (FW 200, specific surface area 280 m²/g, *Degussa*) and alternatively SiO₂ (OX 50, specific surface area 50 m²/g, *Degussa*) with carbon black (Printex 90, specific surface area 460 m²/g, *Degussa*). The silica powders and carbon black were used for the formation of silicon carbide in accordance with Equation (1). The composition of the powder mixtures was chosen so that 5 and 10 vol. % SiC were formed.

To achieve homogenous alumina/silicon-carbide composite precursor powders, it was necessary to obtain well-dispersed slurries containing alumina, carbon black and silicon dioxide. They were prepared by setting the pH value to 10,5 using NH₄OH to get a completely polydispersed slip according to the zeta potentials shown in Fig. 1a, and by using HNO₃ for pH adjustment (pH ≈ 5) and an ethoxylated tallowalkyl amine to get the hydrophobic SiO₂ powder dispersed in water (Fig. 1b). The slurries were homogenized by ultrasonic stirring for 30 min followed by 60 min of agitation ball milling using alumina milling balls.

The slurries were freeze-dried and the powders calcined at 1625°C in a graphite die under flowing argon. Phase analysis of the calcined powders was carried out by XRD using a Bragg-Brentano geometry in a range of 2θ from 20° to 80° with an angle speed of 0,5 °/min and the amount of SiC was determined by means of atom emission spectroscopy. The calcined powders were sieved and then attrition-milled in 2-propanol for 30 min with silicon carbide milling balls (1...2 mm

in size) at a speed of 1200 min⁻¹ in order to break up aggregates formed during reaction calcination. The specific surface area of the resulting powder was measured by the BET method and particle size distribution was measured by static laser light scattering.

The powder samples were uniaxially hot pressed in flowing nitrogen at temperatures of 1700°C for samples with 5 vol. % SiC and 1750°C for samples with 10 vol. % SiC under 35 MPa for one hour. Disk-shaped samples with a diameter of 60 mm were ground to 3,1 mm thickness and then cut into bars with a cross section of 3·4 mm². The bars were prepared in three different states (State I: polishing of test bars to 3 μm finish and bevelling of the edges; State II: annealing (2 h/1300°C/Ar) of the test bars prepared to State I; State III: additional polishing of the lateral sides of the test bars prepared to State I). Testing was carried out in a four-point bending test with an inner span of 10 mm, an outer span of 20 mm at a crosshead speed of 0,1 mm/min. Six to ten beams of each sample were tested.

Fracture toughness was determined on ground and polished samples using the ICL method (Indentation-Crack-Length) using a Vickers indenter at an applied load of 98,1 N.

The fracture surface and the microstructure of sintered, polished and hot-etched samples as well as the morphology of the calcined powders were investigated by means of REM/SEM (6400 F, *Jeol*), whereas TEM (CM-200FEG, *Phillips*) was used to locate the second phase particles within the matrix grains. Therefore the samples were ground, dimpled and thinned by ion beam etching.

3 Results and Discussion

3.1 Powder Characterization

The analysis of XRD diffractograms of calcined powders showed that SiC occurs mainly in the cubic beta modification with a unit cell length of 4,349·10⁻¹⁰ m. A minor amount of less than 10 % of a hexagonal alpha modification was found. The total amount of SiC formed during the calcination process is given in Tab. 1, together with the specific surface areas (ssa) of the composite powders as well as the average particle size distribution by volume of the milled powder. Excess carbon, which occurs due to the fact that gaseous SiO is removed in flowing argon, was burned out at 600 °C for 15 min. In the literature only longer

Tab. 1
SiC content and specific surface areas (ssa) of the calcined powders before and after milling for 30 min in 2-Propanol, d₅₀ is given for the milled powder only (* : prepared with OX 50, other composite powders with R972)

SiC content [vol. %]		ssa before milling [m ² /g]	ssa after milling [m ² /g]	d _{50, Volume} [μm]
intended	effective			
5	4,87	1,46	3,29	2,02
5*	5,01	0,95	3,56	1,66
10	9,99	3,07	5,38	1,97
10*	10,51	2,41	4,59	1,55

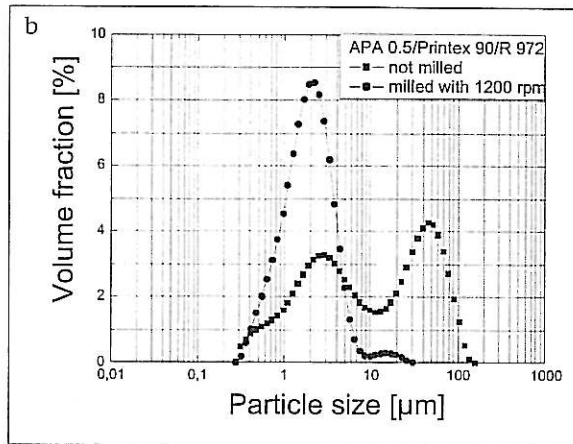
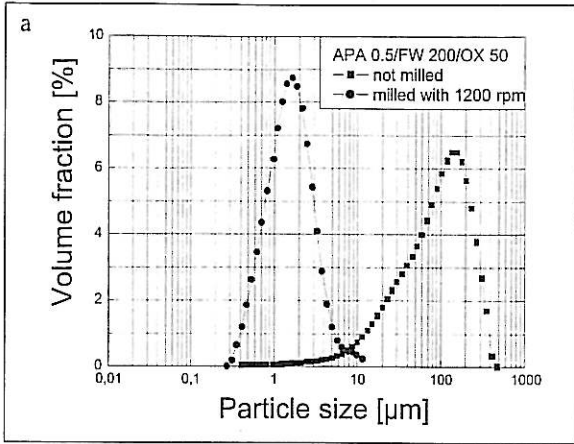


Fig. 2 Particle size distribution of the composite powders with 5 vol. % SiC calcined at 1625°C for the as-calcined and the milled state

times [13] or even higher temperatures [14] could be found for the elimination of excess carbon in the production of SiC powders by carbothermal reduction. After reaction calcination, the specific surface area was around 1 m²/g for powders with 5 vol. % SiC, indicating strong aggregation and/or grain growth compared to the as-received matrix powder (ssa of alumina powder 7 m²/g). After attritor milling for 30 min in 2-propanol with silicon carbide milling balls, the ssa increased up to 3,5 m²/g (Tab. 1) and 5,2 m²/g for the powder with 10 vol. % SiC respectively. The effect of milling can also be shown by examining the particle size distribution of the milled powders in comparison to the as-calcined powders (Fig. 2), which shows that a real comminution could be achieved. But it is also obvious that there are some aggregates left which could not be eliminated by the milling process and require a pressure-assisted densification process.

The system containing FW 200 and OX 50 shows in both cases (before and after milling) a monomodal distribution, whereas the system with Printex 90 and R 972 shows a bimodal distribution before milling. For densification, only milled composite powders with a monomodal particle size distribution were used, which turned out to be suitable for producing composites.

Fig. 3 shows an SEM image of a composite powder containing 5 vol. % SiC. Beside spherical particles, needle-like structures are present. EDX analysis of single needles showed mainly silicon and carbon beside minor amounts of other elements such as Al and O (from the matrix) and Au (from the preparation of the

SEM samples). Small silicon carbide particles were also clearly detectable on alumina grains.

These needle-like crystals are also present in calcined powder mixtures containing only silicon dioxide and carbon black in a molar ratio of 1:3.

The formation of SiC whiskers by using similar starting compositions and process parameters is also described in the literature [15]. According to this work, the morphology of SiC whiskers is controlled by the partial pressures of SiO(g) and CO(g), which occur in the different reaction stages, that are summarized by Eq. (1). In addition, the presence of carbonaceous solid is essential for the formation of needle-like whiskers [15]. Considering the fact, that a graphite die was used for reaction calcinations and taking into account the experimental results presented, it can be concluded that the needle-like crystals are SiC whiskers. Due to the fact that they are randomly dispersed in the calcined powder, the needles are broken by milling and most SiC is existent in spherical shape, the whiskers will have no essential influence on fracture toughness.

3.2 Densification, Microstructure and Mechanical Properties

As described in the experimental part, the composite powders were densified by hot pressing with an uniaxial pressure of 35 MPa. Composite samples with 5 vol. % SiC could be densified at 1700°C for 1 h to relative densities higher than 98 %. But for samples with increased amount of SiC (10 vol. %), an increase

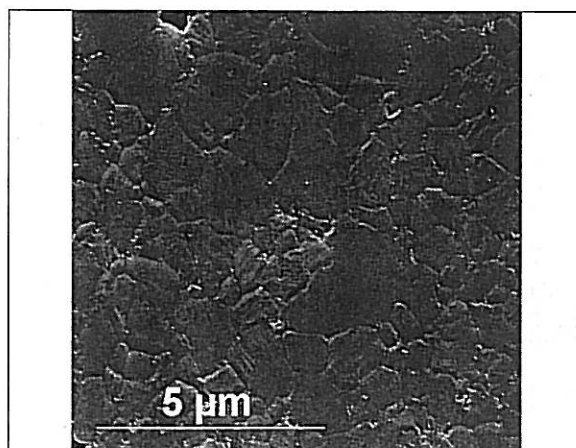
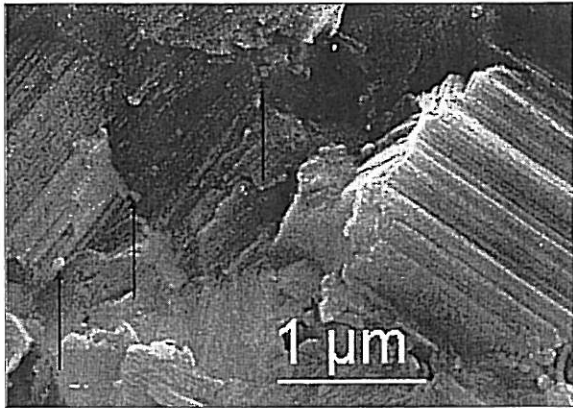


Fig. 3 (left) SEM image of a composite powder containing 5 vol. % SiC after calcination at 1625°C

Fig. 4 (right) Thermally etched cross-section of a composite sample with 5 vol. % SiC (formed with OX 50)

Fig. 5
Fracture surface of a composite sample with 5 vol. % SiC. Arrows indicate some detected SiC particles.



of temperature from 1700°C to 1750°C was necessary to obtain samples with similar density.

The microstructure of the composites was investigated by common SEM and TEM techniques. The grain size of composite samples was around 1,1 μm for both composites with 5 vol. % SiC, 1,04 μm (10 vol. % SiC; prepared with hydrophobic SiO₂) and 0,68 μm (10 vol. % SiC, prepared with hydrophilic SiO₂), respectively. Fig. 4 shows the thermally etched cross-section of a sample with 5 vol. % SiC. The overview of the microstructure shows a homogeneous size distribution of the matrix grains, but also some defects in the μm-range. The formation of these defects can be attributed to aggregates (average particle size 1,5 μm to 2 μm, in contrast to 1 μm average matrix grain size for the hot-pressed composites) which could not be eliminated during milling or hot pressing. At a higher magnification, well-dispersed SiC particles at grain boundaries as well as within the alumina grains can be detected.

All composites show an intragranular fracture mode in contrast to single-phase alumina where the fracture mode is predominantly intergranular. Fig. 5 shows an SEM image of the fracture surface of a composite sample with 5 vol. % SiC. The faceted structure of the fracture surface clearly indicates a fracture along preferred crystallographic directions within alumina crystals. Small SiC particles (< 100 nm) can be detected on the fractured surface. The crack path of the composite samples is illustrated in Fig. 6. Crack deflection, which is caused by grain boundaries or second-phase

inclusions [16], can be observed on grain boundaries as well as within the matrix grains.

Fig. 7 shows a TEM image of a composite sample containing 5 % SiC. Obviously, the silicon carbide particles are located both within the matrix grains and at grain boundaries. The intragranular particles are found to be dominant and their particle size is ≤ 100 nm. Larger SiC particles (> 100 nm) are located at the grain boundaries or at triple points. The grain boundaries as well as triple points are free of glass phase.

The determination of fracture toughness, K_{IC} , with the ICL method, requires knowledge of crack geometry. Depending on the crack system (median/radial cracks or Palmqvist cracks) two different approaches were applied, which lead to different values for K_{IC} . Anja et al. demonstrated that, in alumina/silicon carbide-nanocomposites, Palmqvist cracks are present [17].

Indentations were applied with a Vickers diamond under a load of 98 N both on the polished cross-section of monolithic alumina and alumina/silicon carbide composites. The indented samples were polished again and examined under a light microscope. Fig. 8 shows optical photographs of the polished indents.

In monolithic alumina a continuous crack system is present indicating a median/radial crack system (Fig. 8a). In a composite sample with 5 vol. % SiC, a Palmqvist crack system can be observed, where cracks are no longer connected with the cores of the indentation (Fig. 8b). In order to enable a comparison with other values given in literature, toughness was calculated for both crack systems based on Equations 2 and 3. Ten indentations were made for each sample and crack length was measured immediately after indentation.

median/radial cracks; after Anstis [18]

$$K_{IC} = 0,032 \cdot H \cdot a^{0,5} \cdot (E/H)^{0,5} \cdot (c/a)^{-1,5} \quad (2)$$

Palmqvist cracks; after Niihara [19]

$$K_{IC} = 0,018 \cdot H \cdot a^{0,5} \cdot (E/H)^{0,4} \cdot ((c/a) - 1)^{-0,5} \quad (3)$$

E: Young's modulus [GPa]

H: Vickers hardness [GPa]

a: half of the indentation diagonal length [μm]

l: crack length [μm] and

$c = l + a$ [μm].

The values of K_{IC} are given in Tab. 2. Compared to monolithic alumina (2,53 MPa·m^{0,5}) a slight increase

Fig. 6
Crack paths in samples containing 5 vol. % SiC; prepared with OX 50 (hydrophilic) as the SiO₂ source

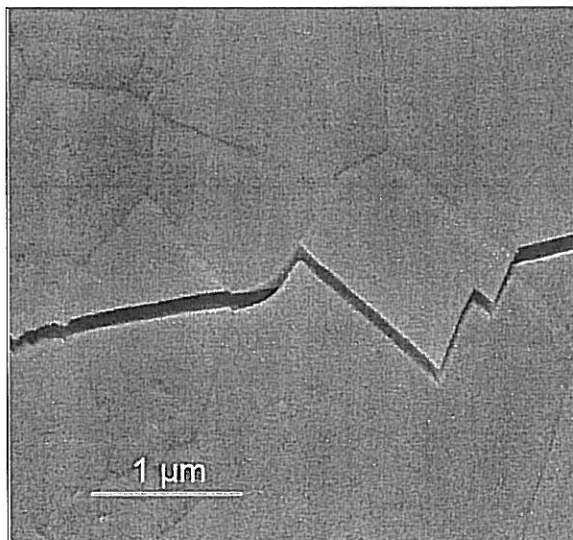
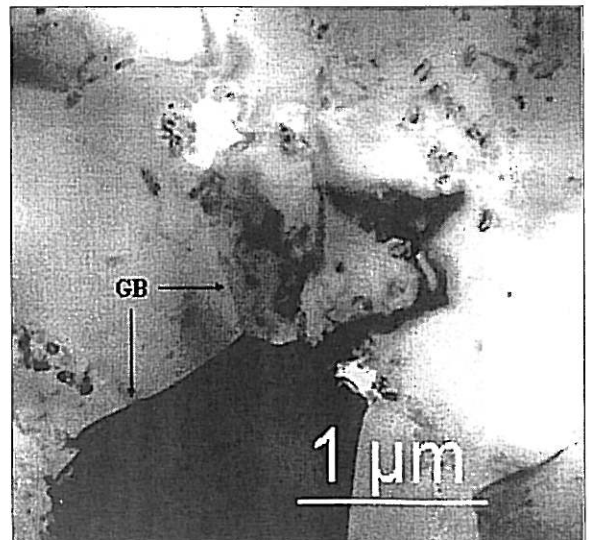


Fig. 7
TEM image of a composite sample containing 5 vol. % silicon carbide



of K_{IC} values for the composite samples (2,63 $\text{MPa}\cdot\text{m}^{0.5}$ for composites prepared with R972 as SiO_2 source and 2,81 $\text{MPa}\cdot\text{m}^{0.5}$ for samples prepared with OX 50) can be obtained using Anstis' approach for the calculation. The composites with 10 vol. % SiC show a similar toughness of 2,62 $\text{MPa}\cdot\text{m}^{0.5}$ and a significant increase in hardness (22 GPa compared to 20,4 GPa for alumina). Using Niihara's correlation (Eq. 3), fracture toughness values 5 $\text{MPa}\cdot\text{m}^{0.5}$ are achieved for all composite samples. Fracture toughness is not affected by an annealing process, so that toughening effects which are triggered by residual stresses induced during machining of the samples, can be excluded.

Fracture strength was measured in four-point bending tests. The values are given in Tab. 2. Looking at the values for composites with 5 vol. % SiC, a significant influence of the SiO_2 source on the fracture strength can be observed, if samples are prepared according to State I. Composites prepared with OX 50 as the SiO_2 source demonstrate a 13-% higher fracture strength (540 MPa) than samples prepared with R972 as the SiO_2 source (474 MPa). Samples with 10 vol. % SiC show significantly lower fracture strength (430 MPa, prep. with R 972; 335 MPa, prep. with OX 50). By polishing the lateral sides of the test bars (Preparation State III), a further strength increase could be achieved with 740 MPa for a composite with 10 vol. % SiC and a matrix grain size of 0,68 μm . In Preparation State I, this composite only reached a strength of 335 MPa. The samples with 5 vol. % SiC reached values of 701 MPa (prep. with R 972) and 635 MPa (prep. with OX 50), when prepared to State III.

The fracture strength also increases significantly by annealing the prepared test bars at 1300°C for 2 h in a flowing argon atmosphere (prep. state II). According to the literature [20], this post-annealing treatment leads to a decrease of internal stresses and an increase in strength. After annealing, there was no significant difference concerning the fracture strength of samples with different SiO_2 sources and samples with different SiC contents.

With regard to a relationship between the SiC content and strength, one has to be aware of the fact that only samples with a similar state of preparation can be compared. In State I, samples with 5 vol. % SiC have a higher strength than those with 10 vol. % SiC, which might confirm the theory of a maximum strength at 5 vol. % SiC. In State II no dependence on the SiC content is evident. With regard to the samples prepared with R 972, they exhibit similar strength values (625 MPa, 5 vol. % SiC and 640 MPa, 10 vol. % SiC), but also similar grain sizes. In State III, it is obvi-

SiC content [vol.-%]	Matrix grain size [μm]	Fracture strength State I [MPa]	Fracture strength State II [MPa]	Fracture strength State III [MPa]	HV ₁₀ [GPa]	K_{IC} (Anstis) [$\text{MPa}\cdot\text{m}^{0.5}$]	K_{IC} (Niihara) [$\text{MPa}\cdot\text{m}^{0.5}$]
0	0,87	377 ± 67	n.d.	n.d.	20,08 ± 0,42	2,53 ± 0,07	n.d.
5	1,12	474 ± 55	625 ± 50	701 ± 97	20,32 ± 0,42	2,63 ± 0,08	4,97 ± 0,07
5*	1,13	540 ± 98	635 ± 18	635 ± 112	20,46 ± 0,25	2,81 ± 0,15	5,12 ± 0,13
10	1,04	430 ± 74	640 ± 71	n.d.	21,95 ± 0,41	2,63 ± 0,15	5,05 ± 0,13
10*	0,68	335 ± 19	850 ± 147	740 ± 160	22,35 ± 0,37	2,62 ± 0,15	5,06 ± 0,13

Tab. 2 Mechanical properties of composites and a reference sample of pure alumina (* prepared with OX50, other composite powders with R972); bold value in column 4: additional polishing of lateral sides before annealing. Weibull modulus is given in brackets (six to ten beams were tested for each sample).

ous that the sample with 10 vol. % SiC (prep. with OX 50) has a higher strength than the sample with 5 vol. % SiC that was also prepared with OX 50. Three relationships between the SiC content and strength are discussed in the literature, a maximum strength at 5 vol. % SiC [1], a continuous climb to a plateau value for strength [21] and the independence of strength of the SiC content [22]. All these researchers used test bars with polished lateral sides, which corresponds to the preparation State III. The strength of the composites prepared with hydrophilic SiO_2 seem to indicate the theory given in [21], but more work has to be done to obtain a clear conclusion.

4 Summary

Carbothermal reduction of silicon dioxide has been applied to produce $\text{Al}_2\text{O}_3/\text{SiC}$ composites with homogeneously distributed nanoscaled SiC. Powder mixtures of Al_2O_3 , SiO_2 and carbon black were calcined at 1625°C and alumina/silicon carbide composite powders with SiC particles of an average particle size of 100 nm were achieved. The amount of SiO_2 and carbon black was selected to obtain composite powders with 5 and 10 vol. % SiC. The SiC particles formed by carbothermal reduction of silicon dioxide consisted of 90 % β -SiC and 10 % α -SiC. Beside spherical SiC particles, a small amount of SiC-whiskers was formed. Due to the high calcination temperature, strong aggregation of the powder was observed, which could be reduced by milling the calcined powder with SiC milling balls.

Composite powders were densified by hot pressing. Composites with a uniform distribution of SiC particles both within the alumina grains and also on the

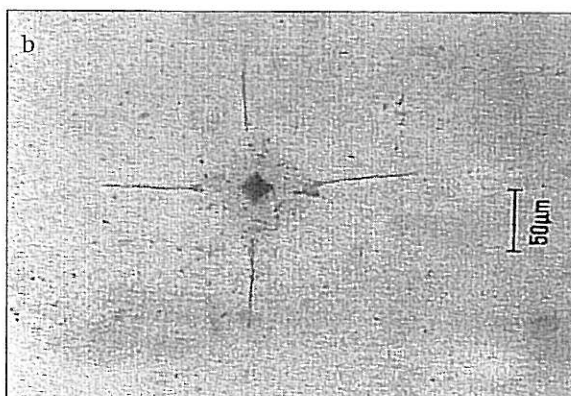
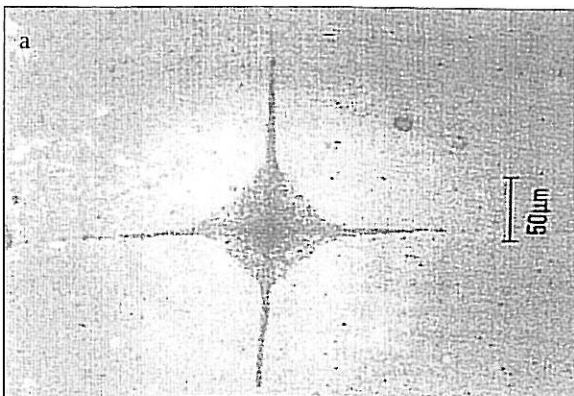


Fig. 8 Vickers indentations in single phase alumina (8a) and in a composite with 5 vol. % SiC (8b) after polishing

grain boundaries were obtained as determined by SEM and TEM investigations. The average grain size of alumina was not affected significantly by 5 vol. % SiC, being 1,1 μm for both composites. Samples containing 10 vol. % SiC have different grain sizes (1,04 μm with R972 as the SiO_2 source and 0,68 μm with OX 50 as the SiO_2 source). The hot-pressed materials exhibited increased fracture strength and fracture toughness in comparison to pure alumina. The average fracture strength increased significantly up to 640 MPa following post-annealing treatment. A maximum strength of 850 MPa, which is an increase of 228 % on that of monolithic alumina, could be achieved by polishing the lateral sides and annealing of the test bars of a sample with 10 vol. % SiC.

5 References

- [1] Niihara, K., New design concept of structural ceramics-ceramic nanocomposites, *J. Ceram. Soc. Jpn.* **99** (1991) 974-982
- [2] Stearns, L.C., Zhao, J. & Harmer, M.P., Processing and microstructural development in Al_2O_3 -SiC nanocomposites, *J. Eur. Cer. Soc.* **10** (1992) 473-477
- [3] Poorteman, M., Descamps, P., Cambier, F., O' Sullivan, D., Thierry, B. & Leriche, A., Optimization of dispersion of nano-size SiC particles into alumina matrix and mechanical properties of corresponding nanocomposite, *Ceramics: Charting the Future*, P.Vincenzini (Ed.), Techna Srl, 1995, 2069-2076
- [4] Carroll, L., Sternitzke, M. & Derby, B., Silicon carbide particle size effects in alumina-based nanocomposites, *Acta mater.* **44** (1996) 4543-4552
- [5] Gao, L., Wang, H.Z., Hong, J.S., Miyamoto, H., Miyamoto, K., Nishikawa, Y. & Torre, S.D.D.L., Mechanical Properties and Microstructure of Nano-SiC- Al_2O_3 Composites Densified by Spark Plasma Sintering, *J. Eur. Ceram. Soc.* **19** (1999) 609-613
- [6] Conder, R.J., Ponton, C.B. & Marquis, P.M., Sol and powder routes to alumina-silicon carbide nanocomposites, *Nano-Structured Materials* **2** (1993) 333-338
- [7] Winn, A.J., Wang, Z.C., Todd, R.I. & Sale, F.R., Alumina-SiC nanocomposites by mixed powder and chemical processing-routes: A preliminary examination of microstructure and response to abrasion, *Silic. Ind.* **63** (1998) 147-152
- [8] Xu, Y., Nakahira, A. & Niihara, K., Characteristics of Al_2O_3 /SiC Nanocomposite Prepared by Sol-Gel Processing, *J. Ceram. Soc. Jap., Int. Ed.* **102** (1994) 312-15
- [9] Sternitzke, M., Derby, B. & Brook, R.J., Alumina/Silicon Carbide Nano-composites by Hybrid Polymer/Powder Processing: Microstructures and Mechanical Properties, *J. Am. Ceram. Soc.* **81** (1998) 41-48
- [10] Sternitzke, M., Review: Structural ceramic nanocomposites, *J. Eur. Ceram. Soc.* **17** (1997) 1061-1082
- [11] Zhao, J., Stearns, L.C., Harmer, M.P., Chan, H.M. & Miller, A.G., Mechanical behaviour of alumina-silicon carbide nanocomposites, *J. Am. Ceram. Soc.* **76** (1993) 503-510
- [12] Chen, C.Y., Lin, C.I. & Chen, S.H., Kinetics of synthesis of silicon carbide by carbothermal reduction of silicon dioxide, *Br. Ceram. Trans.* **99** (2000) 57-62
- [13] Pathak, L.C., Bandyopadhyay, D., Srikanth, S., Das, S.K. & Ramachandrarao, P., Effect of Heating Rates on the Synthesis of Al_2O_3 -SiC Composites by the Self-Propagating High-Temperature Synthesis (SHS) Technique, *J. Am. Ceram. Soc.* **84** (2001) 915-920
- [14] Lee, H.M., Lee, H.L. & Lee, H.J., Submicron Al_2O_3 /SiC Composite Powder Preparation by SHS Technique, *J. Mater. Sci. Let.* **14** (1995) 1515-1517
- [15] Saito, M., Nagashima, S., Kato, A., Crystal growth of SiC whisker from the $\text{SiO}(\gamma)$ -CO system, *J. Mater. Sci. Let.* **11** (1992) 373-376
- [16] Danzer, R., Telle, R., Gefüge und Bruch von Hochleistungskeramikern, Gefüge und Bruch: Werkstoffprüfung 9 Leoben, 31.05.-02.06.1989 Vlg. Bornträger, S. 463-479
- [17] Anya, C.C. & Roberts, S.G., Indentation fracture toughness and surface flaw analysis of sintered alumina/silicon carbide nanocomposites, *J. Eur. Ceram. Soc.* **16** (1996) 1107-1114
- [18] Anstis, G.R., Chantikul, P., Lawn, B.R. & Marshall, D.B., A critical evaluation of indentation techniques for measuring fracture toughness by direct crack measurements, *J. Am. Ceram. Soc.* **64** (1981) 533-538
- [19] Niihara, K., Morena, R. & Hasselman, D.P.H., Evaluation of K_{IC} of brittle solids by the indentation method with low crack-to-indent ratios, *J. Mater. Sci. Let.* **1** (1982) 13-16
- [20] Wu, H.Z., Lawrence, C.W., Roberts, S.G. & Derby, B., The strength of Al_2O_3 /SiC nanocomposites after grinding and annealing, *Acta Mater.* **46** (1998) 3839-3848
- [21] Walker, C.N., Borsa, C.E., Todd, R.I., Davidge, R.W., & Brook, R.J., Fabrication, Characterisation and Properties of Alumina Matrix Nanocomposites, *Br. Ceram. Proc.* **53** (1994) 249-264
- [22] Davidge, R.W., Brook, R.J., Cambier, F., Poorteman, M., Leriche, A., O'Sullivan, D., Hampshire, S., Kennedy, T., Fabrication, properties and modelling of engineering ceramics reinforced with nanoparticles of silicon carbide, *Br. Ceram. Trans.* **96/3**, 1997, 121-127